New method to track length and Differential Wavefront Sensing signals from quadrant photodiodes in heterodyne interferometers with digital PLL readout

Gerhard Heinzel, Nils Brause

Albert-Einstein Institut (Max-Planck Institut für Gravitationsphysik),
Callinstrasse 38, D-30167 Hannover, Germany

E-mail: `gerhard.heinzel@aei.mpg.de`

Abstract. We propose a new method to track signals from quadrant photodiodes (QPD) in heterodyne interferometers that employ digital phase-locked loops for phase readout. Instead of separately tracking the four segments from the QPD and then combing the results into length and Differential Wavefront Sensing (DWS) signals, this method employs a set of coupled tracking loops that operate directly on the combined length and DWS signals. Benefits are increased Signal-to-Noise Ratio in the loops and the possibility to adapt the loop bandwidths to the different dynamical behaviour of length and DWS signals.

1. Introduction

Laser interferometry is a powerful method to measure tiny distance variations as changes of optical pathlengths. When the pathlengths cannot be kept constant to within a small fraction of a wavelength, heterodyne interferometry is frequently applied, i.e. by interfering two laser beams that have a finite frequency difference. The interference pattern is recorded with a photodiode, which produces a photocurrent with a sinusoidal component at the heterodyne frequency. Differential changes of optical pathlength are then converted into phase changes of that sinusoidal beatnote, which are measured with a phasemeter. Several techniques exist to perform this phase measurement[1, 2, 3, 4, 5, 6, 7, 8, 9, 10]. When the heterodyne frequency changes with time, as e.g. in inter-spacecraft interferometers such as LISA[11] or the Laser Ranging Interferometer (LRI) on GRACE Follow-On[10, 12, 13], the usual technique is to employ

a digital Phase-Locked Loop (DPLL)[5, 6, 7, 8, 9, 10, 14] to track the frequency and phase of the beatnote and thus make it available in digital form.

In many applications of laser interferometers, it is beneficial or even essential to determine not only the relative pathlength change between the two interfering beams, but also the angle between their wavefronts, since the latter is a very sensitive measurement of misalignments in the optical system. The standard technique to achieve this angular measurement is Differential Wavefront Sensing (DWS) [15, 16], which uses a quadrant photodiode (QPD) to detect the interference pattern. The average phase over the four segments represents the length signal, while the difference between left and right or top and bottom represent horizontal and vertical misaligments, respectively (see Figure 1).
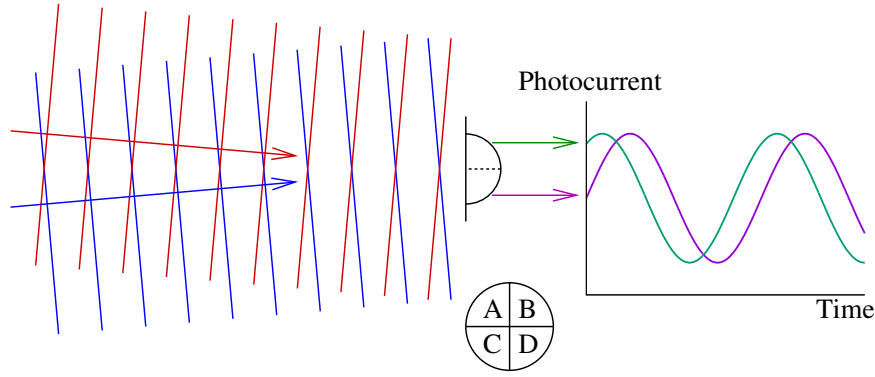

Figure 1. Illustration of Differential Wavefront Sensing.

In previous implementations, the phase measurement is applied separately to each segment of the diode, and the results are then combined. This paper describes a new method to track the phases of the beatnotes from the four segments of a quadrant photodiode with DPLLs. In Section 2, the function of a DPLL as a phasemeter core is summarized. The standard application of four independent DPLLs to the segments of a QPD is described in Section 3, and the proposed new scheme in Section 4. Initial tests are reported in Section 5, followed by a conclusion in Section 6.

2. Phase measurement with Digital Phase-Locked loops

The principle of a Digital Phase-Locked loop is to generate a digital sine wave in a Numerically Controlled Oscillator (NCO), and to make it track the incoming sinusoidal beatnote signal in frequency and phase. After appropriate signal conditioning, the incoming signal is first digitized in an Analog-to-Digital converter (ADC), and all remaining processing happens in the digital domain, typically implemented in a Field-Programmable Gate Array (FPGA) for the tracking part, see Figure 2.

The NCO consists of a Phase Increment Register (PIR) that represents the instantaneous signal frequency, a Phase Accumulator (PA) which holds the integral of the frequency, i.e. the instantaneous phase, and a Look-Up-Table (LUT) that converts
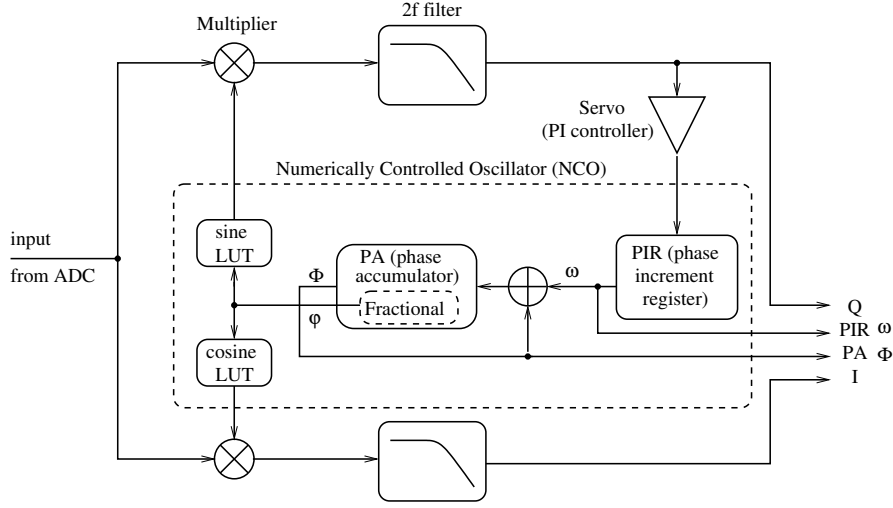
Figure 2. Functional Blocks of a Digital Phase-Locked loop (DPLL).

the phase into a sine wave and optionally also a cosine wave. The ADC and all digital blocks are driven synchronously from a common clock, which sets the reference for any single phase measurement.

In order to make the NCO sine signal track the incoming signal, both are mixed in a multiplier that acts as phase detector, and the phase deviation thus measured is used as error signal in a servo loop. When the loop is closed and locked, both the incoming and the NCO sine signal have the same frequency, and their phase is shifted by 90°, such that their product, the error signal, has zero average. Incoming and NCO sine signal are said to be "in Quadrature" (denoted by 'Q'). An optional second branch multiplies the incoming signal with a digital cosine signal, which is then "In Phase" ('I') and which can be used to measure the amplitude of the incoming signal. Lowpass filters after the mixers suppress the second harmonic of the signal frequency ('$2f$'), a by-product of the multiplication, in order to prevent it from circulating around the loop in an undesired non-linear process. The primary achievement of such a DPLL is that frequency and phase now exist in digital form in the PIR and PA registers, respectively, within the NCO from where they can be directly read out.

More specifically, the PIR holds the instantaneous signal frequency ω in units of cycles per clock period, with $0 < \omega < 0.5$. It slowly varies as the input signal frequency changes. It is integrated in the PA which always has a fractional part φ, with $0 \leq \varphi < 1$ cycles, which is used by the LUTs. It follows a rapid sawtooth function. In most cases, the integer number of cycles (wavelengths) must also be tracked. This can be achieved by including extra bits in the PA that represent the integer number of cycles. We denote that extended PA by Φ, with

$$\varphi = \Phi \bmod 1 \tag{1}$$

simply being the fractional part of Φ. The total phase Φ is an ever increasing ramp. Instead of using extra bits in the PA, the total phase can in principle also

be reconstructed by integrating ω externally.

Among the many performance parameters of a DPLL, most important here is the ability to continuously track the input signal without cycle slips, i.e. integer errors in Φ caused by noise in the input signal. That robustness can be optimized by carefully adapting the servo gain to the dynamics and noise properties of the incoming signal[9, 14, 17].

3. Differential Wavefront Sensing with DPLL phasemeters

If a QPD is used in order to implement DWS, the standard procedure is to connect four independent DPLLs to the four segments A, B, C and D of the QPD. We call their error signals $E_A \ldots E_D$, their PA register contents $\Phi_A \ldots \Phi_D$, and the fractional parts of the latter $\varphi_A \ldots \varphi_D$. They are combined to form the output signals:

$$x = \frac{\Phi_A + \Phi_B + \Phi_C + \Phi_D}{4}, \tag{2}$$

$$\alpha = \frac{\varphi_A - \varphi_B + \varphi_C - \varphi_D}{2}, \tag{3}$$

$$\beta = \frac{\varphi_A + \varphi_B - \varphi_C - \varphi_D}{2}, \tag{4}$$

where x represents the length signal in units of the laser wavelength, and α, β, reduced to the range $-0.5\,\text{cycles} \leq \alpha, \beta \leq +0.5\,\text{cycles}$, represent the horizontal and vertical tilt angles between the wavefronts, scaled by a huge factor that depends on the beam geometry[18]. One more independent linear combination of the segment phases can be formed, which we call the *ellipticity*. It is rarely used but we include it here in anticipation of the next steps:

$$\varepsilon = \frac{\varphi_A - \varphi_B - \varphi_C + \varphi_D}{2}, \tag{5}$$

This scheme is illustrated in Figure 3. Combining the signals according to Equations (2)…(4) is not the only possibility[19]. In LISA Pathfinder[2, 20, 21], for example, x was computed as the argument of a complex vector formed by adding the complex amplitudes from the four segments. This differs from Equation (2) in that the segment contributions are weighted with their respective beatnote amplitude. It is not yet clear which of these alternatives is preferrable with respect to e.g. tilt-to-length cross-coupling. If the segment amplitudes are, however, also measured with the 'I' branch of the DPLL and recorded, the results can be converted into each other in postprocessing.

This standard scheme has been successfully used in many cases, notably for the continuous active alignment over 200 km separation of the inter-satellite interferometer in the LRI on GRACE Follow-On[13]. There, and in other cases like e.g. LISA, it is, however, not optimal:

- The beam divergence over the long distance together with a finite receive aperture results in a very weak received beam (order of 100 pW to a few nW), with resulting
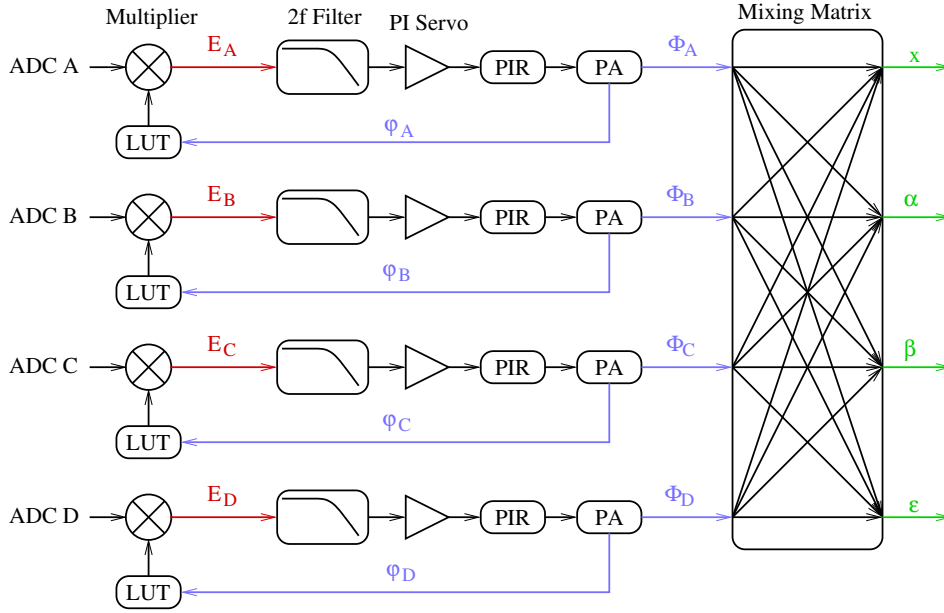
Figure 3. Conventional readout scheme for a Quadrant Photodiode. Each DPLL processes 1/4 of the total signal power which nevertheless has the full dynamics and noise of the length signal.

poor Signal-to-Noise ratio in the heterodyne beat note to be tracked, which limits the achievable robustness of the tracking loops, each of which uses only 1/4 of the total signal power.

- The length signal x has a much higher dynamic range than the angular signals. The former contains the Doppler shift due to the relative spacecraft motion (typically some meters per second, corresponding to some MHz Doppler shifts for a wavelength of about 1 μm), as well as common-mode noise sources such as laser frequency noise, which largely cancel in the other three signals α, β and ε.

- Nevertheless each of the four standard tracking loops contains the full length signal which sets stringent requirements on their loop bandwidths. The resulting open-loop gains are in general not optimal for the much quieter angular signals. The same holds for the $2f$ filters.

- The integer number of cycles, which physically exists only once for each pair of interfering beams, is represented four times in $\Phi_A \ldots \Phi_D$. They should represent the same number of integer cycles and differ only by the small quantities α, β and ε. If, however, a cycle slip occurs in only some of the four segments, the length signal x computed by Equation (2) is easily messed up.

4. New Architecture

In order to overcome the above limitations, we propose here an alternative loop topology, where the four servo loops do not act on the four segments, but on x, α, β and ε instead.

Error signals for these loops can be obtained from Equations similar to (2) to (5):

$$E_x = \frac{E_A + E_B + E_C + E_D}{4}, \tag{6}$$

$$E_\alpha = \frac{E_A - E_B + E_C - E_D}{2}, \tag{7}$$

$$E_\beta = \frac{E_A + E_B - E_C - E_D}{2}, \tag{8}$$

$$E_\varepsilon = \frac{E_A - E_B - E_C + E_D}{2}. \tag{9}$$

The final registers of the four loops track x, α, β and ε, which directly represent the desired final output of the phasemeter. The segment phases, which are still needed for the multiplicative phase detectors, can be easily obtained by inverting Equations (2) to (5):

$$\varphi_A = x + \frac{\alpha + \beta + \varepsilon}{2}, \tag{10}$$

$$\varphi_B = x + \frac{-\alpha + \beta - \varepsilon}{2}, \tag{11}$$

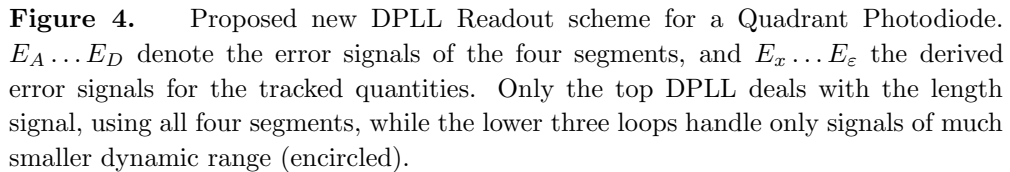$$\varphi_C = x + \frac{\alpha - \beta - \varepsilon}{2}, \tag{12}$$

$$\varphi_D = x + \frac{-\alpha - \beta + \varepsilon}{2}, \tag{13}$$

where only the fractional part of x needs to be used and the results are reduced to the range $0 \ldots 1$ cycles. This scheme is illustrated in Figure 4.

Only E_x carries the burden of the large dynamic range. It uses the combined signal from all four segments, each of which has been coherently demodulated with individually optimized phases. For uncorrelated noise sources, such as shot noise or electronic noise, this yields a 6 dB improvement in Signal-to-Noise Ratio (SNR) which makes the loop more robust against cycle slips. Now there is only one full NCO in the system, which produces the phase ramp Φ and its sawtooth-like fractional part φ, and in particular only one register Φ that keeps track of the integer number of cycles, which better maps the physical reality than having four registers $\Phi_A \ldots \Phi_D$.

The signals in E_α, E_β and E_ε, on the other hand, have a much smaller dynamic range, since both the length signal as well as many noise contributions, such as laser frequency noise or residual intensity noise, largely cancel. Moreover, angular degrees of freedom typically change much slower than e.g. spacecraft separation in cases like LISA or GRACE Follow-On. The outputs of their servo loops are slowly varying numbers with a range that can be limited to e.g. -0.5 cycles $\leq \alpha, \beta, \varepsilon \leq +0.5$ cycles. If physical constraints exist, e.g. from the optical layout, that further limit their actually achievable range, such constraints can easily be implemented by restricting the range of values that the respective registers are allowed to assume, further increasing the robustness. In particular the ellipticity ε will be almost constant in many cases, since it mainly depends on geometrical imperfections of the laser beams.

Each loop can now be individually optimized for the dynamical behaviour and noise characteristics of the corresponding signal. This concerns not only the servo loop

Figure 4. Proposed new DPLL Readout scheme for a Quadrant Photodiode. $E_A \ldots E_D$ denote the error signals of the four segments, and $E_x \ldots E_\varepsilon$ the derived error signals for the tracked quantities. Only the top DPLL deals with the length signal, using all four segments, while the lower three loops handle only signals of much smaller dynamic range (encircled).

bandwidths, but also the $2f$ filters, which can now be made more efficient for the α, β and ε loops.

Going one step further, one could even think of using an optimized Kalman-type estimator for α, β and ε instead of a simple PI controller, and possibly also augment it with guidance information from the respective actuators that are commanded to adjust e.g. the spacecraft attitude or testmass orientation.

At first glance it might seem that this new system could produce fundamentally different outputs, since the mixing matrix that implements Equations (6)...(9) acts on the error signals, which are weighted with the signal amplitudes in the indvidual segments A...D, whereas Equations (2)...(5) act on the phases which have been stripped of the amplitude information. Further analysis shows, however, that this is not the case and that the new system produces the same outputs as the standard one, at least if the servo loops have enough gain and integrator stages to keep all error signals close to zero. In that case, Equations (6)...(9) imply that the segment error signals $E_A \ldots E_D$ are zero as well, which leads to the same outputs as in the standard case. Subtle differences for real signals and loop gains may, however, exist and will be subject of further experimental investigations.

5. Initial tests

Initial tests have been performed using this new architecture in a simple Mach-Zehnder Interferometer. The light sources were two Nd:YAG NPRO lasers phase-locked to each other with 9 MHz offset with separate electronics. The signals were recorded with an InGaAs QPD of 1 mm diameter and were converted to voltages with op-amp based transimpedance amplifiers with 20 MHz bandwidth. The phasemeter operated at 80 MHz clock frequency and used the hardware which is described in Reference [14, Ch. 9]. Other than implementing the mixing matrices shown in Figure 4, the loop parameters were not changed between the old and new schemes. The initial measurements confirmed that the scheme works functionally and is able to determine correct length and DWS signals. The length loop in the new scheme can indeed handle signals of roughly half the amplitude (-6 dB) compared to the standard scheme, both in acquiring the signal and in tracking without cycle slipping, when the artificially increased noise floor remains unchanged, or with the same signal amplitude and 6 dB more noise. Further experiments are being prepared.

6. Conclusion

We have proposed a new scheme to process the heterodyne beatnotes from the four segments of a quadrant photodiode in heterodyne interferometers that use DPLL-based phasemeters. It acts on the length signal x and angular signals α, β and ε, which directly correspond to physically meaningful parameters. The new scheme has advantages in terms of robustness against cycle slips. It allows to individually optimize the loop gains and filter parameters for length and angular signals, which may also lead to lower noise in these outputs. Initial optical experiments have demonstrated the basic functionality, and more detailed experiments are being prepared. We expect that this new scheme may be an attractive alternative for applications like LISA or future GRACE Follow-On-like geodesy missions, as well as possible other applications that employ heterodyne interferometry and need to measure angles in addition to the length signals.

7. References

[1] Cruise A M, Hoyland D and Aston S M 2005 *Classical and Quantum Gravity* **22** S165–S169 ISSN 0264-9381
[2] Heinzel G, Wand V, Garcia A, Jennrich O P, Braxmaier C, Robertson D, Middleton K, Hoyland D, Rudiger A, Schilling R, Johann U and Danzmann K 2004 *Classical and Quantum Gravity* **21** S581–S587 ISSN 0264-9381
[3] Liang Y R, Duan H Z, Yeh H C and Luo J 2012 *Review of Scientific Instruments* **83** ISSN 0034-6748
[4] Pollack S E and Stebbins R T 2006 *Classical and Quantum Gravity* **23** 4189–4200 ISSN 0264-9381
[5] Wand V, Guzman F, Heinzel G and Danzmann K 2006 *LISA phasemeter development* (*AIP Conference Proceedings* vol 873) pp 689–+ ISBN 978-0-7354-0372-7
[6] Shaddock D, Ware B, Halverson P G, Spero R E and Klipstein B 2006 *Overview of the LISA phasemeter* (*AIP Conference Proceedings* vol 873) pp 654–+ ISBN 978-0-7354-0372-7

[7] Gray M B, McRae T, Hsu M T L, Herrmann J and Shaddock D A 2012 *A digital phasemeter for precision length measurements* Conference on Lasers and Electro-Optics ISBN 978-1-55752-933-6

[8] Gerberding O, Sheard B, Bykov I, Kullmann J, Delgado J J E, Danzmann K and Heinzel G 2013 *Classical and Quantum Gravity* **30** ISSN 0264-9381

[9] Francis S P, Lam T T Y, McKenzie K, Sutton A J, Ward R L, McClelland D E and Shaddock D A 2014 *Optics Letters* **39** 5251–5254 ISSN 0146-9592

[10] Bachman B, de Vine G, Dickson J, Dubovitsky S, Liu J, Klipstein W, McKenzie K, Spero R, Sutton A, Ware B and Woodruff C 2017 Flight phasemeter on the laser ranging interferometer on the grace follow-on mission *11th International LISA Symposium* (*Journal of Physics Conference Series* vol 840)

[11] Danzmann K, Lisa Pathfinder Team and eLisa Consortium 2015 *Nature Physics* **11** 613–615 ISSN 1745-2473

[12] Sheard B S, Heinzel G, Danzmann K, Shaddock D A, Klipstein W M and Folkner W M 2012 *Journal of Geodesy* **86** 1083–1095

[13] Joint press release by AEI and NASA/JPL, July 02, 2018; paper in preparation

[14] Gerberding O 2014 *Phase readout for satellite interferometry* Ph.D. thesis Leibniz Universität Hannover URL http://edok01.tib.uni-hannover.de/edoks/e01dh14/783659903.pdf

[15] Morrison E, Meers B J, Robertson D I and Ward H 1994 *Applied Optics* **33** 5041–5049 ISSN 0003-6935

[16] Morrison E, Meers B J, Robertson D I and Ward H 1994 *Applied Optics* **33** 5037–5040 ISSN 0003-6935

[17] Gardner F M 2005 *Phaselock Techniques* (New York: John Wiley & Sons)

[18] Wanner G, Heinzel G, Kochkina E, Mahrdt C, Sheard B S, Schuster S and Danzmann K 2012 *Optics Communications* **285** 4831–4839 ISSN 0030-4018

[19] Wanner G, Schuster S, Troebs M and Heinzel G 2015 A brief comparison of optical pathlength difference and various definitions for the interferometric phase *10th International LISA Symposium* (*Journal of Physics Conference Series* vol 610) URL http://iopscience.iop.org/article/10.1088/1742-6596/610/1/012043/meta

[20] Armano M *et al.* 2016 *Physical Review Letters* **116** ISSN 0031-9007

[21] Armano M *et al.* 2018 *Physical Review Letters* **120** ISSN 0031-9007